Self Consistent Field Calculations of Interactions between Chains Tethered to Spherical Interfaces

Eric K. Lin and Alice P. Gast*

Department of Chemical Engineering, Stanford University, Stanford, California 94305

Received April 19, 1995; Revised Manuscript Received October 6, 1995[⊗]

ABSTRACT: Self consistent mean field (SCF) theory is used to investigate the structure of and interactions between layers of polymer chains tethered to a spherical interface. Traditional methods have combined flat geometry results with the Derjaguin approximation to calculate the interaction potentials between curved surfaces, leading to a great overestimation of both the range and steepness of the pair interaction potential. We have improved upon this approach by utilizing the chain configurational statistics from the curved geometry with a modified Derjaguin approximation to calculate pair interaction potentials. By varying the core radius, the degree of polymerization, and the tethering density in an athermal solvent, the tethered layer assumes structures ranging from those in star polymer systems to planar polymer brushes. The interaction potentials are found to be strictly repulsive with varying degrees of range and steepness. These changes in the interaction potential are related to changes in the tethered layer structure. The results are also compared with those from scaling theories. The range of the interaction potential generally correlates with the layer thickness predicted from scaling theory. The functional form of the interaction potentials does not follow previously proposed forms.

1. Introduction

The interactions between layers of polymer chains tethered by one end are important in many systems including stabilized colloidal suspensions, star polymers, and polymeric micelles. The resulting interaction potentials influence both the microscopic structure and bulk thermodynamic properties of these systems. Tethered polymer chains themselves have also garnered much attention because the polymer configurational statistics differ from those in bulk solution.[1,2] At high tethering densities, the chains overlap, resulting in stretched configurations forming a polymer brush. Most studies to date have focused on polymer brushes at a flat interface since it is the simplest geometry to study. The resulting polymer density profiles and interactions have been investigated theoretically through self consistent mean field (SCF) calculations,[3−7] molecular dynamics simulations,[8] Monte Carlo simulations,[9,10] and scaling analysis.[11,12] These efforts have validated the density profile for a planar polymer layer as approximately parabolic in shape as predicted from the analytic solution to the self consistent mean field equations.[13] Polymer brushes have been studied experimentally using the surface forces apparatus (SFA),[14−16] optical reflectometry,[17] neutron reflectivity,[18,19] and small-angle neutron scattering (SANS).[20−22] These results are also consistent with a parabolic density profile.

In many systems of interest such as colloidal particles or polymeric micelles, polymers are tethered to curved surfaces. The curved interface results in polymer brush structures differing from those at a flat interface due to the increased volume available to the stretched polymer as it moves away from the interface. Tethered chains with curved interfaces have largely been studied in the limiting case of star polymers where they are tethered to a small spherical core. Star polymers have been studied theoretically using scaling arguments,[23] Monte Carlo simulations,[24] and molecular dynamics simulation.[25] Polymeric micelles with small cores can also be described using the star polymer description.[26,27] Scaling theory has shown that the density profile away from the center of the polymer has a power law decay. Less work has concentrated on probing the curvature regime in between the limits of polymer brushes at flat interfaces and star polymers. Dan and Tirrell[28] have performed SCF calculations elucidating the transition between the parabolic polymer brush profile and the star polymer density profile. Wijmans and Zhulina[29] compared lattice SCF calculations to analytic expressions for the density profiles with different curvatures, solvent conditions, and chain lengths. These results are supported by recent Monte Carlo simulation results.[24] Li and Witten[30] have used a variational approach to solve the mean field equations analytically.

Since the tethered layer density profiles change qualitatively with increasing curvature from a parabolic form to a power law decay, one expects the resulting interactions between these structures to change as well. The interactions between polymer layers at curved interfaces have been studied in a number of different contexts. Leibler and Pincus[31] used Flory−de Gennes type arguments to predict intermicellar interaction potentials. Witten and Pincus[32] used scaling arguments to calculate the interactions between colloidal particles stabilized with tethered chains and proposed a logarithmic form for the interparticle potential. Recently, Genz et al.[33] combined the parabolic analytic SCF solution with the Derjaguin approximation to model the structure and thermodynamics of sterically stabilized colloids. The most detailed calculations to date have been performed by Wijmans, Leermakers, and Fleer[34] using the lattice SCF formalism in two dimensions to calculate the interaction potential between stabilized colloidal structures. Due to computational constraints, they were limited to calculation of the interactions between particles with small cores carrying polymer chains having 50 segments.

Experimental studies on polymer layers at curved interfaces have probed monodisperse polymeric micelles and star polymers with scattering techniques. Higgins et al. used SANS to investigate the liquid structure of core-contrast solutions of micelles with increasing concentrations.[35,36] Richter et al.[37] performed similar

[⊗] Abstract published in *Advance ACS Abstracts,* November 15, 1995.

0024-9297/96/2229-0390$12.00/0

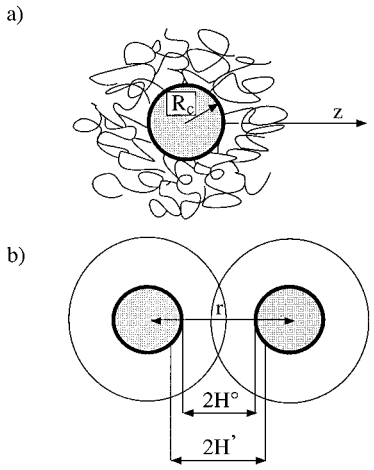

Figure 1. (a) Schematic diagram of the geometry of an isolated particle illustrating the system parameters. (b) Schematic diagram illustrating the variables used in calculating the interparticle interaction potentials.

experiments with star polymers in solution. They were able to observe the liquid structure of the star polymer solution, but at moderate concentrations, the liquid structure is lost when the star polymers completely overlap. Both groups used the Yukawa potential, a model for a screened Coloumbic interaction, as a model pair interaction potential to fit the experimental structure factors. The fits to the experimental data included the use of two adjustable parameters in the potential. Both groups found reasonable agreement with the experimental data, but this approach precludes direct correlation between the polymer layer structure and the resulting interactions.

McConnell et al.[38] have shown conclusively that at moderate solution concentrations polymeric micelles undergo a disorder−order transition into arrays of either body-centered cubic (BCC) or face-centered cubic (FCC) symmetry dependent upon the micellar structure. In a semiquantitative phase diagram, they found that micelles with larger coronal layers relative to the micelle core size favored the BCC array over FCC. The existence of different ordered lattices clearly demonstrates the profound effect of the interactions on the properties of the solution. In an effort to understand the relationship between the tethered chain structure and the intermicellar interactions on the ordering transition, we combined SCF calculations and liquid state theory with SANS experiments on polystyrene−polyisoprene (PS/PI) polymeric micelles in *n*-decane. We found that a one-dimensional SCF calculation with a modified Derjaguin approximation was successful in quantitatively matching measured structure factors.[39]

In this paper we present a theoretical investigation of the interactions between tethered chain layers on curved interfaces. We use the SCF formalism originally developed by Edwards[40] and extended to multicomponent mixtures by Hong and Noolandi[41] and investigate appropriate parameters to examine systematic variations in the interaction potentials with changing physical characteristics. We then compare our findings with the scaling analysis of star polymers in solution.

2. Self Consistent Mean Field Theory

2.1. Isolated Layers. Our goal is to calculate the pair interaction potential between spherical particles with monodisperse tethered chains. We begin by describing the mean field theory for the single-particle case. The system geometry is shown in Figure 1, where R_c is the core radius, σ is the surface number density of the tethered polymer chain, and $\mathbf{z}$ is the radial distance from the core surface. The molecular details of the polymer segments are rescaled so that the polymer is described as a freely jointed chain with N statistical segments of length b.

The fundamental quantity to be calculated in mean field studies is the polymer segment probability distribution function, $G(\mathbf{z},\mathbf{z}'|s)$, representing the probability of finding segment s at the position $\mathbf{z}$, given that the segment started at the position $\mathbf{z}'$. A number of methods are available to solve for G, including lattice methods and continuum approaches. Our description is extracted from the continuum theory developed by Hong and Noolandi.[41]

The polymer chain is modeled as a random walk in a potential field. From this description, the probability distribution function, G, is governed by the forced diffusion equation

$$\frac{\partial G}{\partial s} - \frac{b^2}{6}\nabla^2 G + \omega(\mathbf{z})G = \delta(s)\delta(\mathbf{z} - \mathbf{z}') \qquad (1)$$

where b is the statistical segment length and ω is the mean field potential. In this equation, the connectivity of the polymer chain enters through s and the potential term accounts for the average interaction of one polymer chain with all other polymer chains.

Once G is calculated, the volume fraction profile of the tethered chain layer is described by

$$\phi_A(\mathbf{z}) = \frac{\rho_A(\mathbf{z})}{\rho_{0A}} = \frac{C}{\rho_{0A}W}\int_0^N \mathrm{d}s\; G(\mathbf{z},R_c|s)\int_{R_c}^{\infty}\mathrm{d}\mathbf{z}'\; G(\mathbf{z},\mathbf{z}'|N-s) \qquad (2)$$

where

$$W = \int_{R_c}^{\infty}\mathrm{d}\mathbf{z}'\; G(\mathbf{z}',R_c|N) \qquad (3)$$

is the configurational partition function representing the total number of configurations of a tethered polymer chain, ρ_{0A} is the bulk number density of the polymer, and $\rho_A(\mathbf{z})$ is the local number density at $\mathbf{z}$. Equation 2 can be interpreted as the normalized convolution of two probability distribution functions, one describing a polymer segment of length s, starting at the core surface and ending at the position $\mathbf{z}$, and one describing a polymer segment of length $N - s$ that starts in the bulk and also ends at the position $\mathbf{z}$. The normalization constant C ensures conservation of polymer segments. The solution is assumed to be locally incompressible, and the volume fraction of the solvent is $\phi_S(\mathbf{z}) = 1 - \phi_A(\mathbf{z})$.

The self-consistency in the equations arises from the direct relationship between the volume fraction profiles and the mean field potential, ω, through

$$\omega(\mathbf{z}) = \frac{\rho_{0S}}{\rho_{0A}}\{-\ln \phi_S(\mathbf{z}) + \chi[\phi_S(\mathbf{z}) - \phi_A(\mathbf{z})]\} \qquad (4)$$

where ρ_{0A} is the bulk number density of the chain segments, ρ_{0S} is the bulk number density of solvent molecules, and χ is the Flory−Huggins interaction parameter.[6,41] The mean field potential can be interpreted as the local solvent excess chemical potential and represents the energy associated with replacing a solvent molecule by a polymer segment. This form of

the equation arises from using a local Flory−Huggins free energy density[42] and neglecting higher order concentration gradient terms.

Given the volume fraction profiles from eq 2, the Helmholtz free energy, F, for the tethered chain layer[6] is

$$\frac{F}{kT} = -f \ln W - \rho_{0S}\int_{R_c}^{\infty}[-\ln \phi_S(\mathbf{z}') - \chi\phi_A{}^2(\mathbf{z}')]\, d\mathbf{z}' \quad (5)$$

where k is the Boltzmann constant, T is the temperature, and $f = 4\pi R_c{}^2\sigma$ is the number of chains tethered to the surface. The first term results from the single-chain partition function, and the second term corrects for an overcounting of the segment−segment interactions arising in mean field theories.[43]

Equations 1−5 are solved numerically and the bulk of the computational time involves determining a self-consistent solution for $\phi_A(\mathbf{z})$ and $\omega(\mathbf{z})$ through an iterative procedure. The probability distribution function $G(\mathbf{z},\mathbf{z}'|s)$ is initially set with the ideal random walk solution for the diffusion equation without a potential field and is then used to calculate $\phi_A(\mathbf{z})$ through eq 2. Using $\phi_A(\mathbf{z})$ and $\phi_S(\mathbf{z})$, we solve for the mean field potential $\omega(\mathbf{z})$ and use this in the forced diffusion equation. Equation 1 is solved using a Crank−Nicolson finite difference scheme[44] for $G(\mathbf{z},\mathbf{z}'|s)$ for a given initial condition and boundary conditions, and the procedure is continued until the difference in successive iterations of $\phi_A(\mathbf{z})$ is less than 10^{-8}. Additionally, the generalized secant method[45] is used to accelerate the convergence in a manner similar to that of Hong and Noolandi.[41] Once the volume fraction profiles are calculated, the Helmholtz free energy is easily obtained from eq 5.

2.2. Interacting Layers. Having the relevant equations needed to calculate both the configurational statistics and free energy of an isolated tethered chain layer, we can look at interacting layers. Unlike the one-dimensional isolated layer, the case of interacting spherical particles becomes a two-dimensional problem. To reduce the computational load, we develop approximations for the particle pair interaction potential, $u(r)$, using the equations developed in the earlier section. We improve on the traditional method for calculating the interaction energy between curved surfaces through the Derjaguin approximation[46] where the free energy per unit area from a flat interface geometry is related to the overall curved interaction energy by retaining the configurational statistics in the curved geometry and then applying a modified Derjaguin approximation to calculate the full interaction potential.

To obtain $u(r)$, we first calculate the volume fraction profiles for the interacting layers for a given separation. The volume fraction profiles are calculated for the layers on each particle, and the overall volume fraction for the interacting particles is given by the summation of these two profiles. Then given the mean field potential from eq 4, we iteratively calculate the volume fraction profiles for self-consistency. For a particular separation, we take the resulting profiles to be representative of the chains located on the line joining the centers of the two particles.

Taking advantage of the symmetry of the problem, we integrate over half the separation distance for the Helmholtz free energy per pair of interacting chains as

$$\frac{F(r)}{kT} = -2 \ln W - \frac{2\rho_{0S}}{f}\int_{R_c}^{r/2}[-\ln \phi_S(\mathbf{z}') - \chi\phi_A{}^2(\mathbf{z}')]\, d\mathbf{z}' \quad (6)$$

This Helmholtz free energy is associated with the chains lying along the core center to center line. The local Helmholtz free energy per unit area F_{mid} at the midpoint is then $F(r)\rho_A^{mid}$, where ρ_A^{mid} is the segment number density at the midpoint. The local interaction energy for a given separation ΔF_{mid} is then $F_{mid}(r) - F_{mid}(\infty)$.

Given the local Helmholtz free energy per unit area for different separations, the total interaction potential, $u(r)$, is determined by integrating over the area of overlap at the midpoint in the spirit of the traditional Derjaguin approximation with the equation

$$\frac{u(r)}{kT} = 2\pi \int_{H^\circ}^{R_c+H^\circ}[R_c - H' + H^\circ]\frac{\Delta F_{mid}(H')}{kT}\, dH' \quad (7)$$

where $2H^\circ$ is the core surface to surface separation along the centerline and $2H'$ is the parallel surface separation off the centerline. The range of the interaction potential is then scaled on the particle core diameter.

We now have a set of equations to calculate the interaction pair potentials between spherical particles with tethered polymer chains. By approximating the two-dimensional problem with one-dimensional equations, we have neglected possible lateral redistribution of the polymer segments. As a result, the average segment volume fraction used to calculate the mean field potential may overestimate the actual environment or potential field in a real system. This may not be a bad approximation as the two-dimensional SCF calculations of Wijmans et al.[34] show that the redistribution of the polymer segments is not appreciable until very small separations. Like the traditional Derjaguin approximation, our modified Derjaguin approximation is most accurate for systems where the range of the interaction is small relative to the core radius. We thus expect our calculated interaction potentials to be most accurate for particles with a large core radius relative to the size of the tethered chain layer.

We have saved much computational effort relative to the two-dimensional SCF calculation or a molecular dynamics simulation, allowing us to systematically explore a wide range of systems. We are primarily interested in curvature regimes between the limiting cases of a planar interface and a star polymer. The advantage of using this approach for the interaction potential over the traditional Derjaguin approximation applied to the flat geometry comes from our direct use of the configurational statistics in the curved geometry. The SCF formalism has the additional advantage of describing the details of the polymer configurations within the tethered layers.

3. Results and Discussion

3.1. Theoretical Calculations. In this section, we present both the structure of the tethered polymer layers at spherical interfaces and the resulting interactions between two particles. We aim to study the influence of the polymer layer structure on the interactions by varying the radius of curvature, the degree of polymerization, and the grafting density. To simplify the following analysis, we set $\rho_{0A} = \rho_{0S}$ and $\chi = 0.0$ for an athermal solvent so that comparisons can be made with scaling theories; however, the specific values of these parameters are important for quantitative comparison with experimental systems.[39] The range of the interaction potentials, r, is scaled on the particle core diameter so that different interaction potentials can be compared.

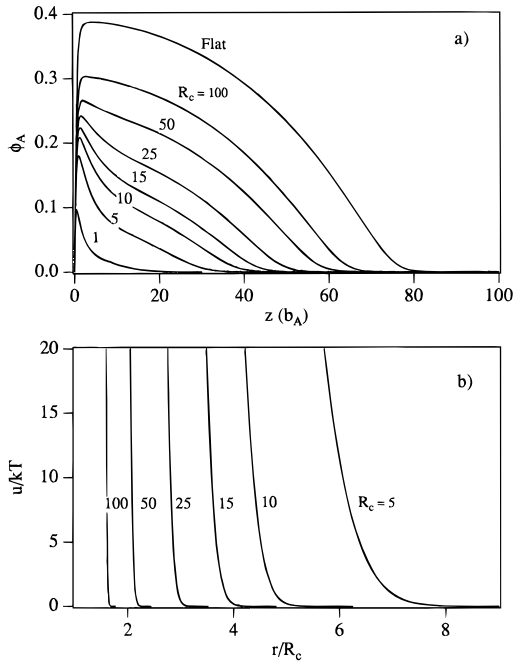

Figure 2. (a) Volume fraction profiles as a function of distance from the interface with $N = 200$, $\sigma = 0.1$, and $\chi = 0.0$ with different values of R_c. (b) The interaction potentials as a function of $r/2R_c$ for the same systems.

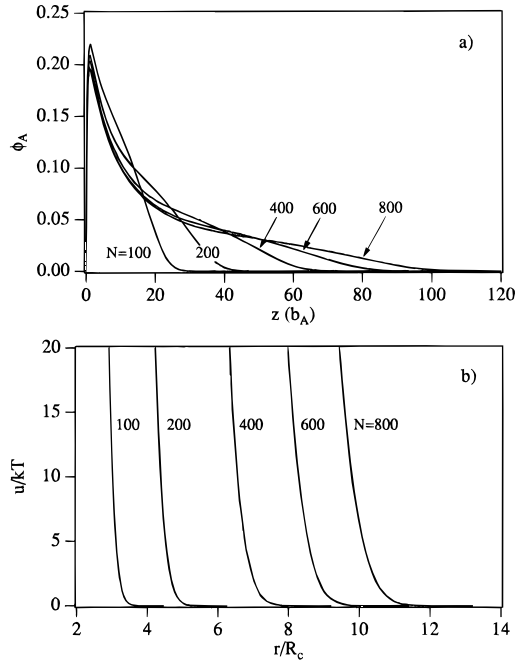

Figure 3. (a) Volume fraction profiles as a function of distance from the interface with $R_c = 10$, $\sigma = 0.1$, and $\chi = 0.0$ with different values of N. (b) The interaction potentials as a function of $r/2R_c$ for the same systems.

The volume fraction profiles for $N = 200$ and $\sigma = 0.1$ with different core curvatures are shown in Figure 2a. These profiles demonstrate the large influence of core curvature on the structure of the tethered chain layer. The shape of the volume fraction profiles smoothly varies from the power law decay of a star polymer when $R_c = 1$ to the parabolic profile characteristic of polymer brushes at a flat interface when $R_c = \infty$. We have made detailed comparisons of our calculations with the volume fraction profiles calculated by Dan and Tirrell[28] and Wijmans and Zhulina[29] and find very good agreement. The equations used here did not involve a virial expansion within the mean field potential and are the continuum analog of the equations used in the lattice calculations. As a result, we find closer agreement with the lattice calculations of Wijmans and Zhulina.

The pair interaction potentials between the polymer layers in Figure 2a are shown in Figure 2b. The interaction potentials are repulsive at all separations with varying degrees of steepness. As for parabolic polymer brushes, the repulsive interaction between the layers arises from the osmotic pressure within the tethered chain layers. The repulsions rise very steeply when the layers come into contact with one another even though the segment volume fraction is very low. This behavior is similar to that of a dilute solution of homopolymers, where random coils behave essentially as hard spheres.[47] As soon as polymer chains begin to overlap, many contacts on the order of kT lead to a strong repulsion. Stronger repulsions are seen for structures with larger R_c because of the rapid increase in the number of polymer chain contacts upon overlap. It is also clear from the profiles in Figure 2a that the use of the planar profile to calculate the interaction potentials for an arbitrary curvature will significantly overpredict both the range and steepness of the interaction. The changes in the polymer layer structure due to the curvature of the tethering interface must be taken into account in order to correctly model the pair interaction potential.

The structure of the polymer layer is also altered through the degree of polymerization N. Figure 3a shows the volume fraction profiles for a particle with $R_c = 10$ and $\sigma = 0.1$ for different N. The volume fraction profiles also change qualitatively from that of a parabolic polymer brush to that of a star polymer as N is increased. Naturally, the structure of the tethered chain layer is determined by the ratio of the size of the polymer layer to the core radius. As the polymer layer extends farther away from the tethering interface, the core curvature becomes less important and the star polymer scaling is recovered. The interaction potentials for these systems are shown in Figure 3b. The range of the interaction is still dictated by the size of the tethered polymer chain layer, and the steepness of the potential also decreases with increasing N as the structure of the particle approaches that of a star polymer. The diminishing steepness of the interaction potential as the system approaches a star polymer arises from the diluteness in the outer edge of the volume fraction profile relative to that of the parabolic brush. When the polymer layers begin to overlap, the polymer segment volume fraction in the layers increases more rapidly for brushlike layers, leading to abrupt increases in the osmotic pressure within the layers. The details in the shape of the volume fraction profiles affect both the range of the interaction through its overall size and the steepness of the interaction through the character of the concentration profile.

Figure 4a shows the volume fraction profiles with $R_c = 25$ and $N = 200$ as the surface density σ increases. Changing the surface density does not effect a change from star polymer behavior to a parabolic polymer brush. Increases in σ primarily result in enhanced stretching of the tethered polymers. This stretching is apparent from increases in both the maximum volume fraction and the size of the polymer layer. The resulting interaction potentials for these systems are shown in Figure 4b. The changes in the range of the interaction follow the differences in the size of the tethered chain layers, but there are not significant changes in the relative steepness of the interactions. Unlike the effect of changing R_c or N, where increases in the brush size were accompanied by a dilution at the outer edges of

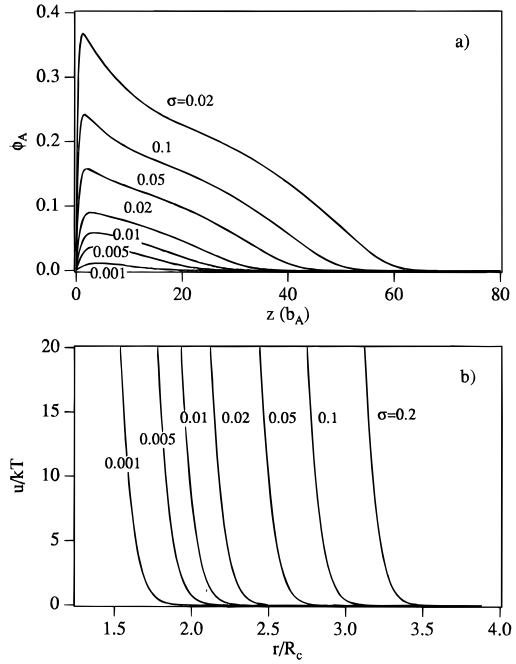

Figure 4. (a) Volume fraction profiles as a function of distance from the interface with $R_c = 25$, $N = 200$, and $\chi = 0.0$ with different values of σ. (b) The interaction potentials as a function of $r/2R_c$ for the same systems.

the profiles, increasing σ leads to enhancements in both the brush density and the thickness.

To compare the range of the pair interactions with scaling theories and other SCF calculations, we characterize the interaction potential energies with the Barker−Henderson effective hard-sphere radius R_{BH} scaled on R_c. This quantity is defined as

$$\frac{R_{BH}}{R_c} = \frac{1}{2}\int_0^\infty dr\,[1 - e^{-u(r)/kT}] \tag{8}$$

and serves as a convenient parameter accounting for the soft-sphere nature of the interaction potentials in a single length scale. The Barker−Henderson effective hard-sphere radius also provides a measure of the total size of a particle with a tethered polymer layer and may be used as a basis for calculating the thermodynamic properties of a suspension.

A good measure for the characteristic size of an isolated tethered polymer layer at a curved surface is given by the second moment of the volume fraction profile

$$H = \left(\frac{\int_{R_c}^\infty \mathbf{z}^2\phi(\mathbf{z})\,d\mathbf{z}}{\int_{R_c}^\infty \phi(\mathbf{z})\,d\mathbf{z}}\right)^{1/2} \tag{9}$$

This measure of the brush size follows the scaling predictions at the appropriate limits and provides a single parameter to describe the brush size that is dependent upon the system parameters.[28,29] The Barker−Henderson hard-sphere radius and the second moment of the isolated brush size can be used to examine both the applicability of the one-dimensional equations for the interaction potential and the limits of different scaling predictions.

We can test the one-dimensional SCF calculations with the modified Derjaguin approximation by comparing with the calculated potentials using the lattice method in two dimensions. Both methods apply a mean field approximation, but the effect of the reduced dimensionality can be approximately assessed in relation to the two-dimensional treatment.[34] The lattice calculations have small errors associated with the use of a cylindrical grid resulting in slight mismatches in placing a spherically symmetric particle within it. These errors are larger near the tethering interface but are small at the outer edge of the volume fraction profile. The values for R_{BH} and H for tethered polymer layers for $N = 50$, $\sigma = 0.1$, and different R_c are shown in Table 1. For these systems, the results of the one-dimensional SCF calculations compare favorably with the two-dimensional ones. As expected, agreement is best when the size of the polymer brush layer is near the size of the core radius. Greater discrepancies are seen in systems with greater curvature because the modified Derjaguin approximation becomes less applicable and the lateral redistribution of chains is more important. As a result, the one-dimensional calculations result in a larger R_{BH} relative to that of the two-dimensional lattice calculations.

Table 1. Comparison of the SCF Calculations Using the Derjaguin Approximation with the Two-Dimensional SCF Results Using the Barker−Henderson Hard-Sphere Radius R_{BH} and Ratio of the Second Moment of the Calculated Polymer Volume Fraction Profile, H, to the Core Radius

core radius R_c	1-D SCF R_{BH}/R_c	2-D SCF R_{BH}/R_c	1-D SCF H/R_c
2.0	5.20	4.59	3.93
5.0	3.62	3.15	2.36
10.0	2.40	2.34	1.74

From Figures 2−4, it is clear that the form of the segment volume fraction profiles over each parameter range differ from one other, but the interaction potentials demonstrate that the structure of outer edges of the tethered polymer structures primarily determines the pair interaction potentials. The interaction between two particles does not greatly perturb the polymer segment volume fraction profile because the tethered chain layers have very strong repulsions with small overlapping distances. At the locally dilute or semidilute volume fractions within the layers, mean field theory becomes less applicable because it neglects correlations between polymer segments by averaging the mean field potential. At these conditions, scaling theory becomes the more appropriate theoretical tool. Scaling theory provides information about the appropriate length scales in a polymer solution but does not describe the local structure nor the shape of the volume fraction profile. Scaling analysis has been used to describe tethered chain structures for both star polymers and polymer brushes, and the consistency of the SCF results with the scaling theories can be evaluated at both curvature limits. Deviations from the scaling limits at intermediate curvatures can also be determined using the numerical calculations.

3.2. Comparison with Analytic Predictions. Scaling theories describe the behavior of semidilute polymer solutions by introducing the idea of "blobs" with a diameter defined by the correlation length, ξ, and energy kT, within which a polymer chain does not interact with other chains.[42] Using closely packed blobs, the solution can be treated via polymer melt statistics to obtain the properties of polymeric solutions and tethered chain structures. In terms of the different core curvatures that we study, scaling analysis is most appropriate to tethered polymer layers that are large relative to the core radius, while mean field theory will be more applicable for thinner tethered polymer layers.

The scaling model for star polymers or polymers tethered to a small spherical particle was developed by both Daoud and Cotton[23] and Birshtein and Zhulina.[48] The polymer layer is modeled as a series of concentric rings of blobs growing in size with radial distance due to the increase in the available volume for each polymer chain. The tethered polymer chains are assumed to be stretched so that each chain end is located in the outer blob at the edge of the polymer layer. The number of blobs within each concentric ring is simply the number of tethered chains at the core interface, and the size of the star polymer is determined from requiring polymer segment conservation. Using this model in a good solvent, the size of the tethered polymer layer, H, scales as

$$H \sim N^{3/5}\sigma^{1/5}R_c^{2/5} \tag{10}$$

To make quantitative comparisons for particles with intermediate curvatures, the above scaling model was extended to polymeric micelles by Cogan et al.[27] In this model, diblock copolymer micelles were modeled using the star polymer description, with additional constraints imposed by the micellar structure. The overall particle radius in a good solvent, R_{part}, is given by

$$R_{part} = \left[\frac{8N(4\pi\sigma)^{1/3}R_c^{2/3}}{3\cdot 4^{5/3}\cdot(3/5)} + R_c^{5/3}\right]^{3/5} \tag{11}$$

As expected, the results from this model were in better agreement with experimental data for polymeric micelles with core radii smaller than the tethered chain layer than for micelles with larger core radii.

Since we are interested in curvatures between that of the star polymer system and the polymer brush, the scaling predictions for the parabolic polymer brush will also be useful for comparison. These relationships, given by Alexander[11] and de Gennes,[12] show that the size of a brush in a good solvent scales as

$$H \sim N\sigma^{1/3} \tag{12}$$

Again, the scaling analysis assumes that all of the polymer chain ends are located equidistant from the interface, resulting in a step volume fraction profile. The scaling theory is useful to determine how the layer size changes with each system parameter but cannot provide more detailed information about the interactions. A better structural description is given by the analytic solution to the SCF equations for polymer brushes at a flat interface in the limit of infinite N and moderate σ, resulting in a volume fraction profile which is parabolic is shape.[13] The size of the particle, R_{plane}, is then given by $R_c + H$. The scaling relationships established from the step profile model are still valid for the parabolic brush. These relationships provide us with simple equations to see if the numerical SCF results are consistent with the analytic results at the corresponding limits and to evaluate when the scaling or parabolic results are appropriate.

It is of interest to see if the range of the particle interaction potential scales in the same way as the brush height. The range of the interaction potential from the tethered polymers is given by subtracting the core contribution to the effective hard-sphere radius, $R_{BH}/R_c - 1$. This quantity is shown as a function of N for different R_c in Figure 5. For small R_c, the core has a small effect and the range of the interaction scales in a similar manner as the star polymer case; however,

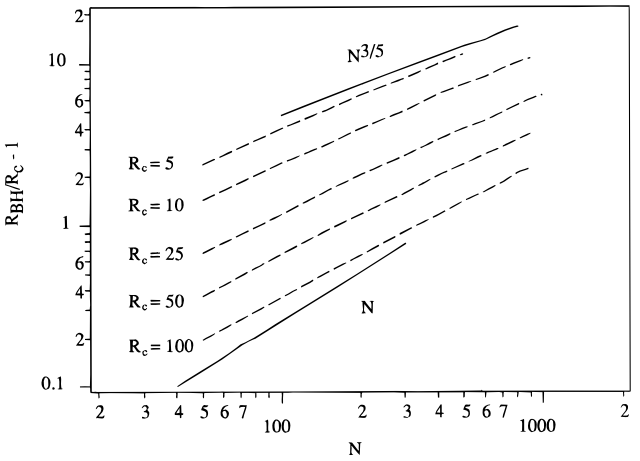

Figure 5. Effective layer size from the interaction potentials given by $R_{BH}/R_c - 1$ as a function of the degree of polymerization. The scaling predictions for a star polymer and a polymer brush are given by the solid lines.

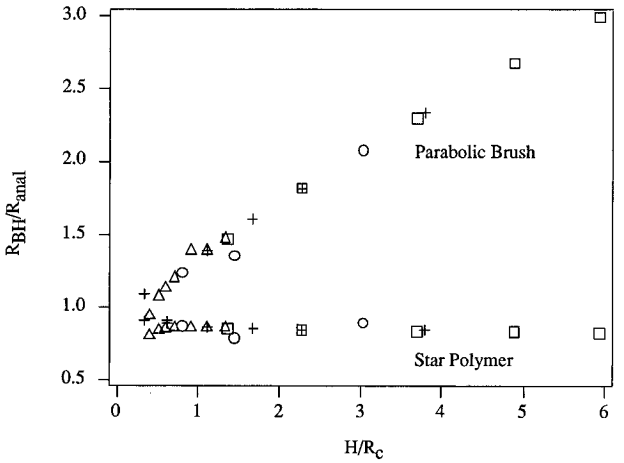

Figure 6. Analytic predictions for the overall radius of the particle scaled on the calculated Barker−Henderson effective hard-sphere radius as a function of the ratio of the second moment of the calculated volume fraction profile to the core radius for the calculations for the potentials from Figure 2 (+), Figure 3 (□), Figure 4 (△), and Table 1 (○).

there are still deviations from the star polymer scaling even for systems with a small core radius. For larger R_c, the interactions nearly follow the scaling predictions for the planar parabolic brush. At larger values of N, the scaling should gradually approach that of a star polymer as the effect of the core interface decreases. In a similar manner to the scaling of the polymer layer size, the range of the interparticle interactions roughly follows the scaling laws at the expected limits; however, scaling laws are not able to provide good predictions for the interaction range at inrtermediate curvature ranges. The softness in the interaction potentials does not greatly perturb the Barker−Henderson hard-sphere radius from the scaling relationships for the polymer layer size.

The applicability of the analytic predictions for the range of the interaction can be determined from Figure 6, which plots the calculated Barker−Henderson hard-sphere radius normalized by the predicted values of the overall particle size from the analytic models versus the ratio of the second moment of the polymer layer profile to the core radius. This plot is similar to one by Dan and Tirrell[28] used to determine the brush size to core radius ratio at which the flat geometry results are effectively recovered. The analytic results are applicable for a system of interest when R_{BH} is equal to

the analytic predictions. For this condition to hold, the particles effectively interact as hard spheres with a radius given by the overall particle size. The points within Figure 6 represent the predictions for parameters representative of all of the calculations presented earlier.

The values for R_{BH} from the numerical SCF potentials are bracketed by the overall size of the particles given by the star polymer scaling, R_{part}, and the parabolic profile prediction, R_{plane}. For large values of H/R_c, the starlike micelle predictions are much closer to the SCF value of R_{BH} than the planar prediction. This illustrates the large error associated with using a flat geometry to predict the overall size of the particle with a tethered chain layer, up to a factor of 3 for particles with $H/R_c \approx 6$. For small values of H/R_c, the planar parabolic description for the effective interaction range is nearer to the numerical SCF values. Naturally, the planar description is more adequate for a system with weak curvature. Over the entire parameter range, the quantitative scaling model by Cogan et al.[27] consistently predicts an effective range of interaction that is ≈80% of the SCF Barker−Henderson hard-sphere radius; this discrepancy is largely due to a greater amount of polymer chain stretching predicted from the SCF calculations. Although the scaling theory makes a large assumption regarding the location of the polymer chain ends, the model is adequate over a range of curvatures and parameter values.

Scaling theory is useful in determining guidelines for the range of the interaction but is unable to provide a specific form for the interaction potential needed to predict specific thermodynamic and structural properties of solutions of these particles. Witten and Pincus[32] have proposed a form for the interaction potential between spherical particles with tethered polymer chains based upon the Daoud−Cotton description of a star polymer and suggest that the interaction potential scales with the free energy of a single tethered chain layer through

$$\frac{u(r)}{kT} \sim 4\pi R_c^3 \sigma^{3/2} \ln(r/R_{part}) \qquad (13)$$

including a logarithmic dependence of the potential on the separation distance. The SCF interaction potentials calculated here do not have a logarithmic form. This difference is not surprising because the scaling model assumes that the free energy of two interacting particles each with f tethered chains can be approximated by the free energy of one particle with $2f$ chains. As a result of this assumption, the scaling model interaction energy does not arise from the specific interaction between the two polymer layers and does not take into account changes in the brush structure and the related changes in the correlation lengths from the enhanced concentrations occurring with polymer layer overlap. The SCF calculations show that the interactions rise very steeply and the particles do not approach the small separation distances attained in the scaling model. The scaling model does demonstrate that more tethered short chains will lead to steeper repulsions than fewer longer chains. Shorter polymer chains reduce the diluting effect of the spherical geometry and result in a polymer layer structure more like the parabolic brush while a higher grafting density results in smaller blobs, increasing the number of kT contacts between interacting layers at a given separation distance. These changes in the profiles are demonstrated in the SCF calculations.

Other functional forms for the interaction potential between tethered chain layers have been suggested, including the Yukawa potential with an exponential decay[36,37] and an analytic form based upon the parabolic profile.[33] We were not able to fit the SCF potentials with a Yukawa potential because the Yukawa potential does not decay rapidly enough. Genz et al.[33] used the parabolic profile to calculate an interaction potential. This form of the interaction potential overestimates the range and steepness of the interaction potentials. Genz et al. do show that even these steeply rising potentials cannot be replaced by substituting an effective hard-sphere interaction to calculate both the structure and properties of suspensions of these particles with tethered chain layers, illustrating the importance of accurately calculating the details of the interaction potentials.

There is no scaling expression able to collapse all of the interaction potentials onto a single curve. The difficulty arises from the lack of a single defined length scale or energy scale for each particle size since the scaling relationships are only valid at their respective limits. The scaling length for the size of the polymer layer changes from the planar description to the star polymer description in a manner yet to be determined. The scaling predictions are useful in examining limiting behavior and provide general guidelines for the ranges of the interaction potentials but are not adequate to describe both the structure and interactions between tethered chain layers on spherical particles.

4. Conclusion

The interface curvature is an important parameter in tethered chain structures as it changes the configurational statistics of the polymer chains and consequently the tethered chain layer structure and interactions. We have performed numerical SCF calculations using a spherical geometry in conjunction with a modified Derjaguin approximation to calculate both the pair interaction potentials and the segment volume fraction profiles. Unlike traditional methods in which the flat interface segment profiles are used to calculate the interaction potentials for particles with curvature, we employed the configurational statistics directly from a curved geometry. We neglected any lateral redistribution of polymer segments when the polymer layers begin to interact and used a modified Derjaguin approximation relating a local Helmholtz free energy per area to the interparticle interaction potential function. These assumptions significantly decreased the computational load and are most appropriate for particles with a small range of interaction relative to the core radius.

We have calculated the volume fraction profiles and interaction potentials for different core radii, grafting densities, and degrees of polymerization in a good solvent. Varying these parameters, the structure of the tethered chain layer can be changed from systems resembling a star polymer to that of a parabolic polymer brush. The resulting interaction potentials are repulsive at all separations with different degrees of steepness. Parabolic brush layers produce shorter ranged steeper interaction potentials, while star polymer-like structures interact via longer ranged less steep potentials. The character of the interaction potentials reflects the tethered layer structure. Steeper potentials result from the rapid increase in the polymer segment volume fraction upon overlap for more brushlike structures. Longer range interactions arise from the star polymer-like structures because of the larger layer size relative

to the core radius. These calculations also demonstrate the larger errors involved with using volume fraction profiles from a flat interface to calculate the interaction potentials for particles with an arbitrary curvature.

The interaction potentials were characterized through the Barker−Henderson effective hard-sphere radius, providing a single length scale taking into account the soft-sphere nature of the potentials. We have shown that the results from the one-dimensional SCF treatment are in good agreement with those from a two-dimensional SCF lattice calculation. This effective hard-sphere radius provides a good measure of the range of interaction and was used to compare the SCF calculations with predictions from scaling theory and the analytic solution to the mean field equations.

In general, the interaction potentials are steeply repulsive, corresponding to an overlap of only the outer edges of the tethered chain layers before reaching an effectively hard-sphere interaction energy. Since the interaction potentials are primarily dictated by the dilute outer edges, scaling theory becomes appropriate at these concentrations although it is unable to provide detailed information about the specific tethered chain layer structure. The numerical SCF results were compared with models for the polymer brush and star polymers to check the consistency of the calculations with scaling at semidilute concentrations and to evaluate the scaling predictions in intermediate curvature regimes. We find that the calculated interaction range is bracketed by the predictions from the two curvature limits. The parabolic profile overpredicts the range of the interaction, with greater discrepancies for systems with a polymer layer size larger than the core radius. The star polymer predictions consistently underestimate the SCF results.

A number of functional forms have been proposed to model interactions between tethered chain layers at curved interfaces, including a logarithmic decay from a scaling analysis, a Yukawa potential with an exponential decay, and an expression from parabolic brush equations combined with the Derjaguin approximation. The calculated interaction potentials are not adequately fit with any of these potential forms. It is not surprising that the interaction potentials cannot be scaled to a single universal function because there is no single length scale valid for all curvatures.

The SCF calculations have been successful in quantitatively matching experimental structure factors in diblock copolymer micellar suspensions with tethered chain layers with intermediate curvatures.[39] SCF theory can adequately model experimental data without having to incorporate adjustable parameters into an interaction potential form or to undertake computationally demanding two-dimensional SCF calculations or numerical simulation techniques. Scaling theory and analytic solution to the SCF equations can provide an estimate of the range of the interaction potentials but are only appropriate at their respective limits. The theoretical formulation presented here can be easily extended to include polydisperse chains, free polymers within the solution, multicomponent chains, or interactions between particles with different core radii.

Acknowledgment. E.K.L. thanks the National Science Foundation for fellowship support. This work was supported in part by the MRSEC Program of the National Science Foundation under Award No. DMR-9400354.

References and Notes

(1) Milner, S. T. *Science* **1991**, *251*, 905.
(2) Halperin, A.; Tirrell, M.; Lodge, T. P. *Adv. Polym. Sci.* **1992**, *100*, 31.
(3) Cosgrove, T.; Heath, T.; van Lent, B.; Leermakers, F.; Scheutjens, J. *Macromolecules* **1987**, *20*, 1692.
(4) Dolan, A. K.; Edwards, S. F. *Proc. R. Soc. London, A* **1974**, *337*, 509.
(5) Dolan, A. K.; Edwards, S. F. *Proc. R. Soc. London, A* **1975**, *343*, 427.
(6) Whitmore, M. D.; Noolandi, J. *Macromolecules* **1990**, *23*, 3321.
(7) Wijmans, C.; Scheutjens, J. M. H. M.; Zhulina, E. B. *Macromolecules* **1992**, *25*, 2657.
(8) Murat, M.; Grest, G. *Phys. Rev. Lett.* **1989**, *63*, 1074.
(9) Chakrabarti, A.; Toral, R. *Macromolecules* **1990**, *23*, 2016.
(10) Lai, P. Y.; Binder, K. *J. Chem. Phys.* **1991**, *95*, 9288.
(11) Alexander, S. *J. Phys. (Paris)* **1977**, *38*, 983.
(12) de Gennes, P.-G. *Macromolecules* **1980**, *13*, 1069.
(13) Milner, S. T.; Witten, T. A.; Cates, M. E. *Macromolecules* **1988**, *21*, 2610.
(14) Tirrell, M.; Patel, S.; Hadziioannou, G. *Proc. Natl. Acad. Sci. U.S.A.* **1987**, *84*, 4725.
(15) Taunton, H. J.; Toprakcioglu, C.; Klein, J. *Macromolecules* **1988**, *21*, 3333.
(16) Taunton, H. J.; Toprakcioglu, C.; Fetters, L. J.; Klein, J. *Nature* **1988**, *332*, 712.
(17) Leermakers, F.; Gast, A. *Macromolecules* **1991**, *24*, 718.
(18) Cosgrove, T.; Heath, T. G.; Phipps, J. S.; Richardson, R. M. *Macromolecules* **1991**, *24*, 94.
(19) Field, J. B.; Toprakcioglu, C.; Ball, R.; Stanley, H.; Dai, L.; Barford, W.; Penfold, J.; Smith, G.; Hamilton, W. *Macromolecules* **1992**, *25*, 434.
(20) Cosgrove, T.; Ryan, K. *Langmuir* **1990**, *6*, 136.
(21) Auvray, V.; Auroy, P. Scattering at Interfaces: Variations on Porod's Law. In *Neutron, X-Ray, and Light Scattering*; Lindner, P., Zemb, T., Eds.; Elsevier Science Publishers: Amsterdam, Netherlands, 1991; pp 199−221.
(22) Auroy, P.; Mir, Y.; Auvray, L. *Phys. Rev. Lett.* **1992**, *69*, 93.
(23) Daoud, M.; Cotton, J. P. *J. Phys. (Paris)* **1982**, *43*, 531.
(24) Toral, R.; Chakrabarti, A. *Phys. Rev. E* **1993**, *47*, 4240.
(25) Grest, G. S.; Kremer, K.; Witten, T. A. *Macromolecules* **1987**, *20*, 1376.
(26) Vågberg, L. J. M.; Cogan, K. A.; Gast, A. P. *Macromolecules* **1991**, *24*, 1670.
(27) Cogan, K. A.; Capel, M.; Gast, A. P. *Macromolecules* **1991**, *24*, 6512.
(28) Dan, N.; Tirrell, M. *Macromolecules* **1992**, *25*, 2891.
(29) Wijmans, C. M.; Zhulina, E. B. *Macromolecules* **1993**, *26*, 7214.
(30) Li, H.; Witten, T. *Macromolecules* **1993**, *27*, 449.
(31) Leibler, L.; Pincus, P. A. *Macromolecules* **1984**, *17*, 2922.
(32) Witten, T. A.; Pincus, P. A. *Macromolecules* **1986**, *19*, 2509.
(33) Genz, U.; D'Aguanno, B.; Mewis, J.; Klein, R. *Langmuir* **1994**, *10*, 2206.
(34) Wijmans, C. M.; Leermakers, F. A. M.; Fleer, G. J. *Langmuir* **1994**, *10*, 4514.
(35) Higgins, J. S.; Dawkins, J. V.; Maghami, G. G.; Shakir, S. A. *Polymer* **1986**, *27*, 931.
(36) Higgins, J. S.; Blake, S.; Tomlins, P. E.; Ross-Murphy, S. B.; Staples, E.; Penfold, J.; Dawkins, J. V. *Polymer* **1988**, *29*, 1968.
(37) Richter, D.; Jucknischke, O.; Willner, L.; Fetters, L.; Lin, M.; Huang, J.; Roovers, J.; Toporovski, C.; Zhou, L. L. *J. Phys. IV* **1993**, *3*, 3.
(38) McConnell, G. A.; Gast, A. P.; Huang, J. S.; Smith, S. D. *Phys. Rev. Lett.* **1993**, *71*, 2102.
(39) McConnell, G. A.; Lin, E. K.; Gast, A. P.; Huang, J. S.; Lin, M. Y.; Smith, S. D. *Faraday Discuss. R. Soc. Chem.* **1994**, *98*, 121.
(40) Edwards, S. F. *Proc. Phys. Soc.* **1965**, *85*, 613.
(41) Hong, K. M.; Noolandi, J. *Macromolecules* **1981**, *14*, 727.
(42) de Gennes, P.-G. *Scaling Concepts in Polymer Physics*; Cornell University Press: Ithaca, NY, 1979.
(43) Russel, W. B.; Saville, D. A.; Schowalter, W. R. *Colloidal Dispersions*; Cambridge University Press: Cambridge, Great Britain, 1989.
(44) Carnahan, B.; Luther, H. A.; Wilkes, J. O. *Applied Numerical Methods*; John Wiley and Sons: New York, 1969.
(45) Wolfe, P. *Commun. ACM* **1959**, *2*, 12.
(46) Derjaguin, B. V. *Kolloid Z.* **1934**, *69*, 155.
(47) Flory, P. J. *Principles of Polymer Chemistry*; Cornell University Press: Ithaca, NY, 1953.
(48) Birshtein, T. M.; Zhulina, E. B. *Polymer* **1984**, *25*, 1453.

MA9505282